JMEPEG (2012) 21:1879–1884
DOI: 10.1007/s11665-011-0099-6

1059-9495/$19.00

Electrodeposition and Corrosion Properties of Zn-V_2O_5 Composite Coatings

S. Bindiya, S. Basavanna, and Y. Arthoba Naik

(Submitted April 4, 2011; in revised form September 2, 2011)

Composite coatings were obtained by electrochemical codeposition of V_2O_5 nanoparticles with zinc, from an additive free acid sulfate bath. The corrosion behavior of electrodeposited Zn and Zn-V_2O_5 composite coatings was investigated in 3.5% NaCl solution using polarization and electrochemical impedance spectroscopy (EIS). The decrease in I_{corr} values and an increase in R_{ct} values show the higher corrosion resistant nature of Zn-V_2O_5 coatings. The observed textural modifications of composite coatings are associated with the specific structural modification of Zn crystallites provoked by the adsorption-desorption phenomena occurring on the metal surface, induced by the presence of V_2O_5 nanoparticles. It has been observed that the presence of V_2O_5 nanoparticles favors the [1 0 2] and [1 1 2] texture of zinc matrix. Moreover, the codeposition of V_2O_5 nanoparticles with zinc was found to be favored at pH 3.5 and applied current density 4 A dm^{-2}. A considerable grain refinement of the deposit occurred due to incorporation of V_2O_5 nanoparticles and hence improved the preferred orientation of the zinc crystallites.

Keywords composite coatings, corrosion, electrodeposition, Zn-V_2O_5

1. Introduction

Zinc is recognized as an excellent sacrificial coating for ferrous materials and is commonly applied on steel surfaces by electrodeposition (Ref 1-4). Recently, significant interest has been generated in the fabrication of zinc composite coatings via electrodeposition in which ceramic particles or fibers are incorporated into metal matrix. In order to extend the area of application of zinc, many investigators have tried to improve its strength and corrosion resistance by alloying it with hard particles, such as SiO_2, Al_2O_3, ZrO_2, TiO_2, and carbon nanotubes, etc. (Ref 5-11). However, these nanoparticles agglomerated very easily in the plating bath because of its high surface energy; the agglomeration of these particles in the plating bath would correspondingly result in enhanced amount of agglomerated particles in composite coatings, which also results in the disappearance of unique properties of composite coatings. Therefore, fabrication of metal-ceramic composite coatings by cathodic electrodeposition requires the use of stable suspensions of positively charged ceramic particles. Surfactants are generally used in electroplating solutions to improve distribution of particles and to facilitate the deposition of composite coatings (Ref 12-14).

The vanadium oxide particles have attracted tremendous interest from fundamental and perspective. The V_2O_5 nanoparticles have many potential applications in various industrial and domestic fields including metallic and composite coatings. It has also been used to reinforce metallic coatings and it improves wear resistance, hardness, and other properties such as corrosion resistance. However, very few investigations have been made on the corrosion behavior of V_2O_5-metal composites.

In the present work, we have conducted a study on the elctrodeposition of Zn-V_2O_5 from sulfate bath. Specifically, we investigated the microhardness and the effect of applied current density on corrosion behavior of zinc coatings embedded with V_2O_5 nanoparticles.

2. Experimental

2.1 Reagents

All the chemicals used for electrodeposition were of analytical grade. L-Cystiene was purchased from Merck Ltd., and ethylene glycol was procured from Himedia Pvt. Ltd. Zinc sulfate ($ZnSO_4 \cdot 7H_2O$), sodium sulfate (Na_2SO_4), boric acid (H_3BO_3), ammonium metavanadate (NH_4VO_3), and cetyl trimethyl ammoniumbromide (CTAB) were obtained from S. D. Fine Chemicals Ltd. Double distilled water was used for the preparation of bath solutions.

2.2 Preparation of V_2O_5 Nanoparticles

Vanadium pentoxide (V_2O_5) nanoparticles were prepared by hydrothermal method. In a typical procedure, ammonium metavanadate and L-cystine were dissolved in 5 mL hot water under constant stirring (molar ratio 1:1). A total 35 mL solution balanced with ethylene glycol was transferred into a 50 mL in volume Teflon-lined stainless steel autoclave. Hydrothermal treatment was carried out at 200 °C for 2 h in a furnace. After that, the autoclave was cooled to room temperature and the product was collected, washed with double distilled water followed by alcohol and dried in a hot air oven. The resulting

S. Bindiya, S. Basavanna, and **Y. Arthoba Naik**, Department of Chemistry, School of Chemical Sciences, Kuvempu University, Shankaraghatta 577451, India. Contact e-mail: drarthoba@yahoo.co.in.

yellow powder was calcined at 550 °C for 3 h. The obtained V_2O_5 nanoparticles were characterized and used for the composite coatings.

2.3 Electrodeposition of Composite Coatings

Electrodeposition of pure zinc and Zn-V_2O_5 coatings were carried out from acid sulfate bath under stirred condition. The constituents of the bath were optimized through Hull cell experiments. The basic bath composition and deposition condition are shown in the Table 1. Prior to the plating, V_2O_5 nanoparticles were well dispersed in the electrolyte by subjecting the bath solution to stirring for 24 h. The cathode used was mild steel (4×4 cm^2) and anode was pure zinc (99.99%). The mild steel specimens were polished mechanically and degreased in trichloroethylene followed by water wash. The surface area of anode and cathode was activated by dipping in 10% HCl for few seconds followed by water wash.

2.4 Polarization and Electrochemical Impedance Studies

The polarization and impedance measurements were carried out using CHI660D electrochemical workstation. The composite coated steel specimen was used as working electrode. Platinum wire and saturated calomel electrodes were used as auxiliary and reference electrodes, respectively. The sample surface (working electrode) area exposed to the electrolyte was about 1 cm^2. To begin the measurements, the electroplated sample was rinsed with double distilled water introduced into the cell immediately and was allowed to attain a steady-state. The anodic dissolution of deposit was conducted in a voltammetric mode at a potential scan rate of 5 mV s^{-1}. The values of electrochemical corrosion parameters, the corrosion potential (E_{corr}), and corrosion current (I_{corr}) were measured for the samples obtained at different deposition current densities.

The AC impedance measurements were carried out in the frequency range of 1 mHz to 100 KHz, at the rest potential, by applying 5 mV sine wave AC voltage. The interfacial double layer capacitance (C_{dl}) and charge transfer resistance (R_{ct}) were obtained from simple Randles equivalent circuit. The stimulation program (SIM) was used to build the circuit to get the required parameters. A Nyquist plot is obtained by plotting the real part (Z') and an imaginary part (Z'') of an impedance vector.

Table 1 Optimum bath composition and operating parameters

Bath composition	Optimum quantity, g L^{-1}	Operating conditions
$ZnSO_4 \cdot 7H_2O$	240	pH: 3.5
$Na_2SO_4 \cdot 6H_2O$	40	Temperature: 298 K
H_3BO_3	10	Current density: 4.0 A dm^{-2}
V_2O_5	1.0	Deposition time: 10 min
CTAB	0.5	

2.5 SEM and XRD Studies

The surface morphology of V_2O_5 nanoparticles and the deposits were studied, using SEM, Model JEOL-JSM-35 LF at 25 kV. SEM images of the coated specimens with pure zinc and zinc composite coatings were used to assess their surface morphology. The XRD patterns of the deposits were recorded using Philips (TW 3710) X-ray diffractometer.

2.6 Microhardness Measurements

The Vickers microhardness of the coatings was determined by an indentation technique with a weight of 100 g for 10 s using microhardness tester. Each sample was tested for five times and the average value was calculated.

3. Results and Discussion

3.1 Characterizaion of V_2O_5 Nanoparticles

Figure 1(a) shows the XRD pattern of V_2O_5 nanoparticles prepared by the hydrothermal process. The *d*-spacing and *hkl* values are well indexed to a pure orthorhombic phase of V_2O_5 (JCPDS No: 84-2422]. No characteristic peaks arising from possible impurities are detected. This indicated the high purity

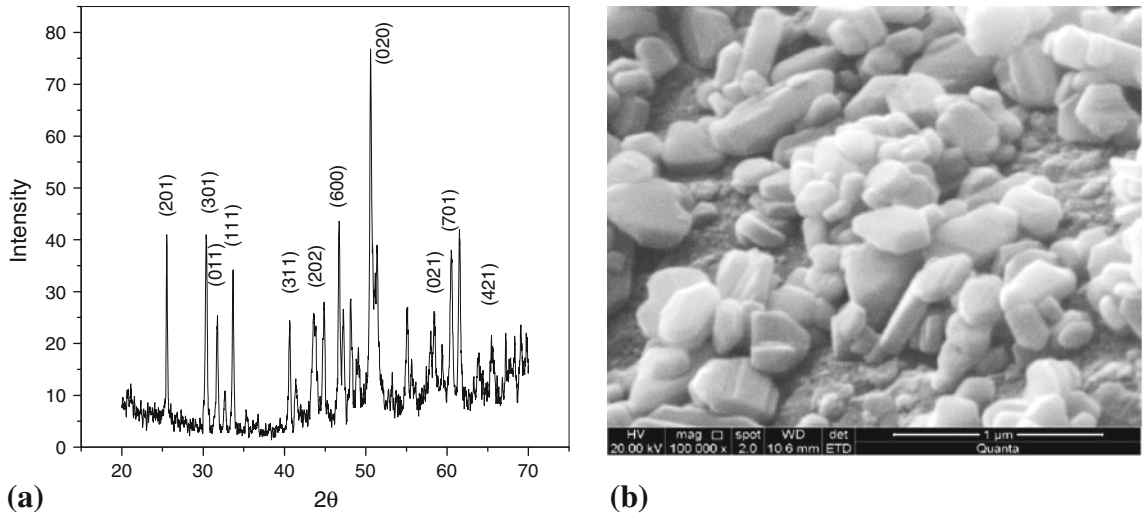

Fig. 1 X-ray diffraction pattern (a) and SEM image of V_2O_5 nanoparticles (b)

of the electrodeposited composite. The average crystallite size as calculated from XRD line broadening using Scherrer's formula was 33 nm. The prepared V_2O_5 nanoparticles exhibit clusters consisting of strips, with typical dimensions are shown in Fig. 1(b).

3.2 Polarization Studies

Figure 2 shows the Tafel plots of Zn and Zn-V_2O_5 composite coatings in 3.5% NaCl solution. The corrosion potential (E_{corr}) and corrosion current (I_{corr}) were calculated from Tafel plots and presented in Table 2. The result indicated that the composite coating obtained from the bath containing V_2O_5 nanoparticles and at the current density of 4 A dm^{-2} exhibits the best corrosion resistance. The E_{corr} and I_{corr} values of the composite coatings were found to be −1.005 V and 109 μA cm^{-2}, respectively, illustrating a significant improvement in corrosion resistance over the pure zinc coatings. It is considered that when V_2O_5 nanoparticles are embedded in the zinc matrix, the corrosion path is more distorted as compared to pure zinc coating, which is favorable for corrosion resistance. Also, the formation of fine grained structure due to the codeposition of V_2O_5 nanoparticles promotes good corrosion resistance as compared to coarse-grained structure of pure zinc (Ref 15, 16).

3.3 Electrochemical Impedance Studies

Figure 3 shows the Nyquists plots of zinc and Zn-V_2O_5 composite coatings measured in 3.5% NaCl solution. An electrical double layer (C_{dl}) exists on the interface between the electrode and the surrounding electrolyte. Charge transfer resistance (R_{ct}) is the resistance offered by the metal atom to get ionized when in contact with the electrolyte. A solution resistance (R_s) between the reference electrode and working electrode has been measured, which represent the resistance of ions in the electrolyte transferring to the electrodes (Ref 17). The fitted parameters for the coatings were presented in Table 2. The Zn-V_2O_5 composite coatings exhibit bigger radius compared to that of zinc coating, which indicated the better corrosion resistance of Zn-V_2O_5 composite coatings. The increase in R_{ct} value is observed and it was maximum at 4 A dm^{-2}. This is attributed to the increase in hardness of compact microstructure of composite coatings. While increase in the deposition current density the zinc content in the deposit increased with a decrease in the R_{ct} value. These EIS results confirmed the higher corrosion resistance of Zn-V_2O_5 composite coatings which in good agreement with the polarization studies.

3.4 SEM and XRD Studies

Figure 4 shows the surface morphology of pure zinc and Zn-V_2O_5 deposits obtained at varying current densities. The SEM image of the zinc deposit shows the hexagonal zinc crystallites oriented nearly parallel to the substrate. The SEM photomicrograph of Zn-V_2O_5 deposit obtained at the deposition current density of 2 A dm^{-2} shows coarse-grained deposit having non-uniform crystal size (Fig. 4b). The distribution of

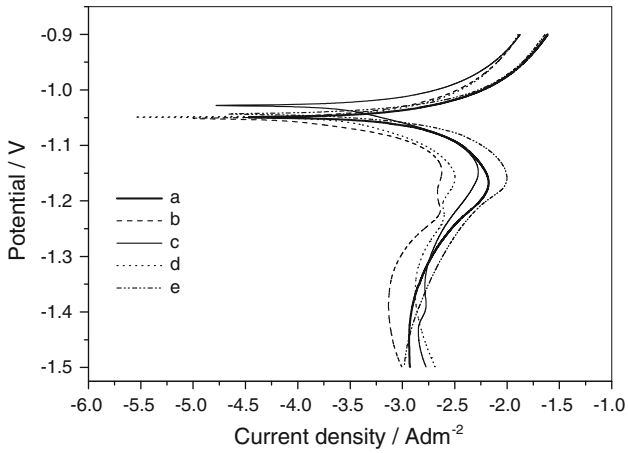

Fig. 2 Potentiodyanamic polarization studies of (a) pure zinc deposited at 4 A dm^{-2} and Zn-V_2O_5 composite coatings at (b) 2 A dm^{-2}, (c) 4 A dm^{-2}, (d) 6 A dm^{-2}, and (e) 8 A dm^{-2}

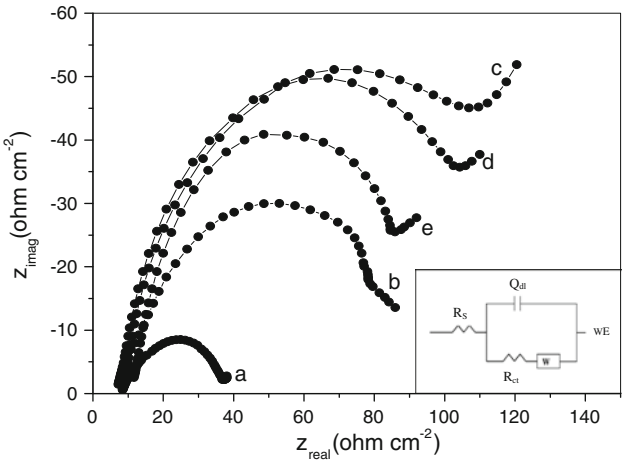

Fig. 3 Nyquists plots for (a) pure Zn deposited at 4 A dm^{-2} and Zn-V_2O_5 composite coatings at (b) 2 A dm^{-2}, (c) 4 A dm^{-2}, (d) 6 A dm^{-2}, and (e) 8 A dm^{-2}. Inset is the Randles equivalent circuit

Table 2 Polarization and EIS parameters of Zn and Zn-V_2O_5 composite coatings obtained from Fig. 2 and 3

Sample	Current density, A dm^{-2}	E_{corr}, V	R_p, Ω cm^2	I_{corr}, μA cm^{-2}	R_{ct}, Ω cm^{-2}	C_{dl}, μA cm^{-2}	Curves in Fig. 2 and 3
Zn	4	−1.091	14	317	68	2.45	a
Zn-V_2O_5	2	−1.077	23	187	83.8	2.20	b
	4	−1.005	48	109	189	1.12	c
	6	−1.090	24	146	136	1.53	d
	8	−1.330	21	165	94.2	1.87	e

V_2O_5 nanoparticles in the deposit shows a marked difference at 4 A dm^{-2} (Fig. 4c). Increase in the deposition current density to 6 A dm^{-2}, increases crystal size, refinement regulates the uniform arrangement of crystals and hence results in the fine-grained deposits (Fig. 4d). Further increase in the current density to 8 A dm^{-2}, there was no significant changes observed in the surface morphology of the composite coatings (data not shown).

The XRD patterns of zinc and Zn-V_2O_5 composite coatings were represented in Fig. 5. The analysis of the diffractograms shows an increase in intensity of the peak in composite coated sample than that of pure zinc coating. This fact is associated to a modification of zinc deposition, which improves after the incorporation of V_2O_5 nanoparticles (Ref 18).

The preferred orientation of zinc electrodeposits was estimated from the X-ray data according to the methodology developed by Muresan (Ref 19, 20), where the texture coefficient (T_c) is calculated by using the equation:

$$T_c(hkl) = \frac{I_{(hkl)}}{\sum I_{(hkl)}} \times \frac{\sum I_{0(hkl)}}{I_{0(hkl)}} \times 100$$

where $I_{(hkl)}$ is the peak intensity of the alloy/composite electrodeposits, $\sum I_{(hkl)}$ the sum of intensities of the independent peaks. The index '0' refers to the intensities for the standard zinc powder sample.

The calculated texture coefficients are plotted in Fig. 6. The Zn-V_2O_5 composite coatings show significant value of T_c than pure zinc coating. In presence of V_2O_5 nanoparticles a modification in the crystallographic orientation of zinc crystallites occurs. In case of pure zinc deposit, 20.03% of zinc crystallites are oriented parallel to (102) plane and 28.76% are

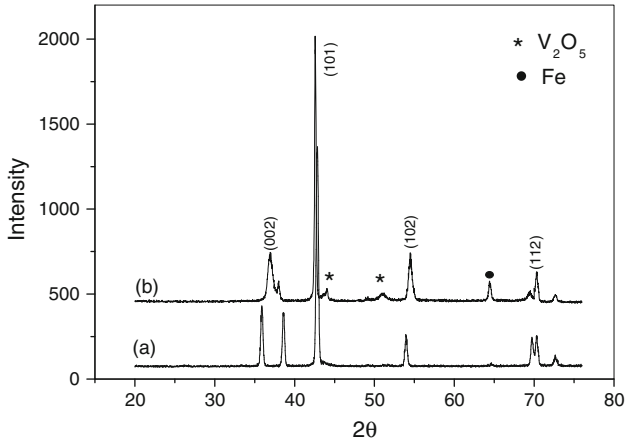

Fig. 5 X-ray diffraction patterns of: (a) Zn and (b) Zn-V_2O_5 composite coatings deposited at current density 4 A dm^{-2}

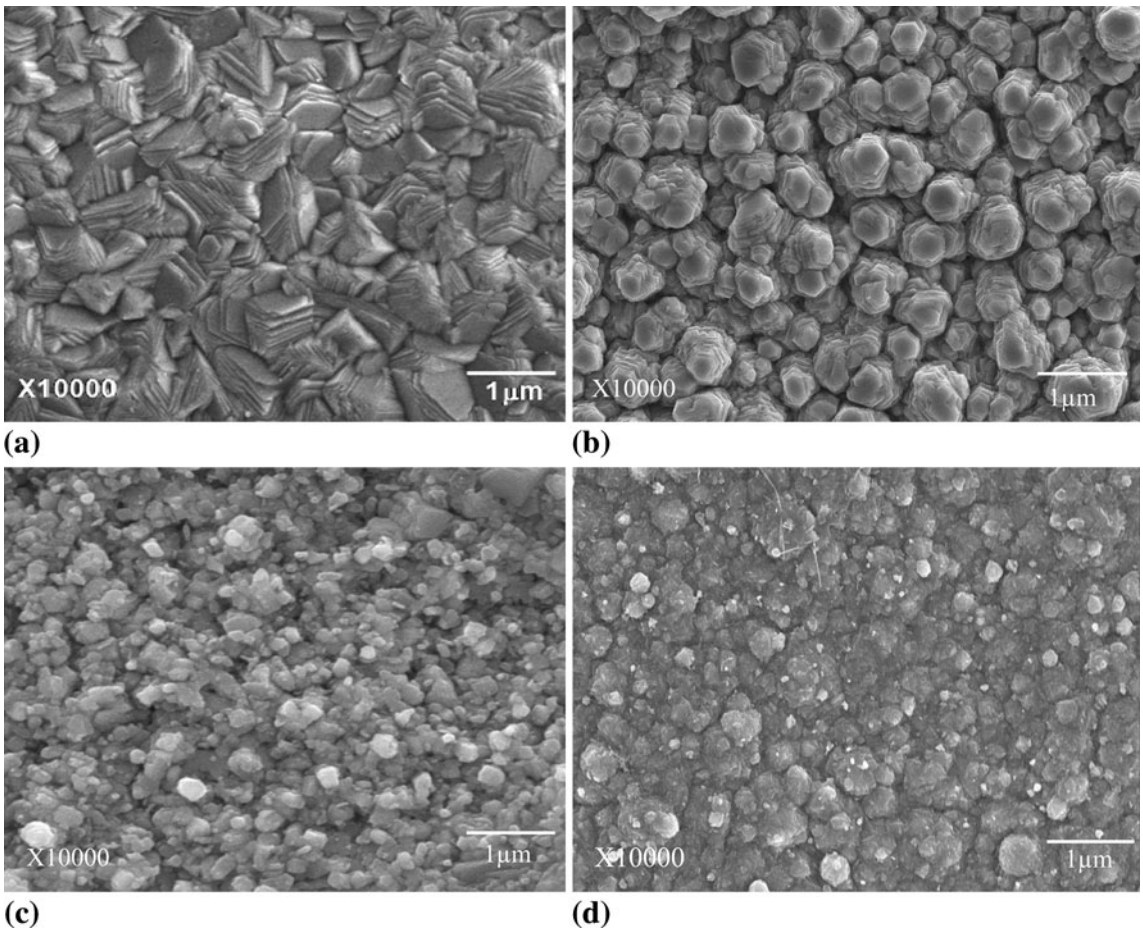

Fig. 4 SEM photomicrographs showing the surface morphology of (a) pure zinc deposited at 4 A dm^{-2} and Zn-V_2O_5 coatings deposited at (b) 2 A dm^{-2}, (c) 4 A dm^{-2}, and (d) 6 A dm^{-2}

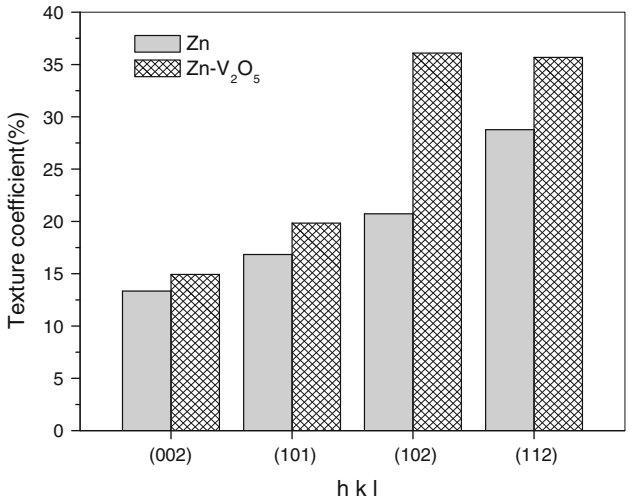

Fig. 6 Preferential orientations of Zn and Zn-V_2O_5 composite coatings

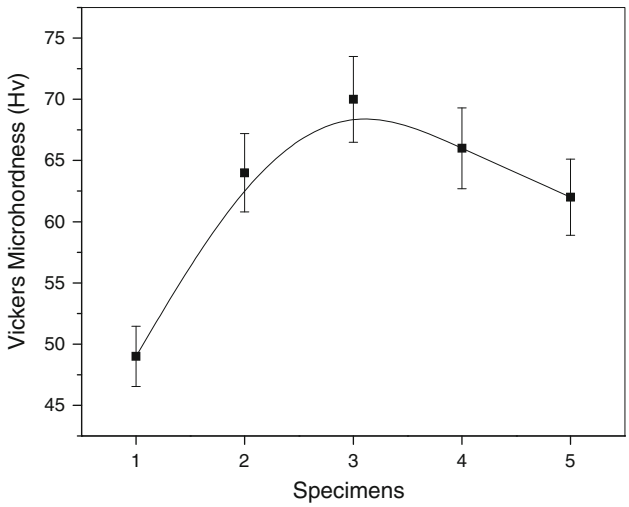

Fig. 7 Microhardness values of specimens (1) pure Zn deposited at 4 A dm^{-2} and Zn-V_2O_5 composite coatings at (2) 2 A dm^{-2}, (3) 4 A dm^{-2}, (4) 6 A dm^{-2}, and (5) 8 A dm^{-2}

oriented parallel to (112) plane. In case of Zn-V_2O_5 composite coatings, 36.09% are oriented parallel to (102) crystallographic plane and 35.68% are oriented parallel to (112) crystallographic plane. Hence, these results indicated that in presence of V_2O_5 (102) and (112) planes are the preferred crystallographic orientations.

The above results revealed that the incorporation of V_2O_5 plays a remarkable influence on the preferred orientation of the metal matrix as a consequence of the changes on metal deposition mechanism. This result is in accordance with that stated in the literature (Ref 21, 22), that the particles embedded in the coatings can affect the preferred orientation of the metallic matrix.

3.5 Microhardness Measurements

The microhardness measurements were performed on pure Zn and Zn-V_2O_5 composite coatings prepared at different applied current densities (Fig. 7). The microhardness of the composite coatings increased with the incorporation of V_2O_5 nanoparticles into the zinc matrix. It was observed that the microhardness value found to be high at the applied current density of 4 A dm^{-2}. While increasing the current densities the microhardness has slightly decreased which may be attributed to the increase in Zn% in the deposit. The increased hardness of the coatings increases the load carrying capacity and improves the resistance for plastic deformation. Nanoparticles in the deposit will also hinder the movement of the dislocation, which increases the microhardness of the composite and suppresses the recrystallization and growth of crystal grains (Ref 23).

4. Conclusion

1. Nanosized V_2O_5 particles were prepared successfully by hydrothermal method. The crystallite size was calculated from X-ray diffraction patterns. The SEM images showed the nanostrips with a typical dimension.
2. Zn-V_2O_5 composite coatings have been deposited from the acid sulfate bath containing V_2O_5 nanoparticles.
3. The microhardness of Zn-V_2O_5 composite coatings varied with the plating current density and it was observed that Zn-V_2O_5 prepared at low current density of 4 A dm^{-2} exhibited higher hardness value of 70 Hv.
4. The calculated texture coefficients for Zn-V_2O_5 composite coatings showed that the presence of V_2O_5 in the plating bath play a significant influence on the preferred orientation of the metal matrix. The preferred crystallographic orientations of Zn-V_2O_5 composite coatings were (102) and (112) planes.
5. The polarization and EIS measurements showed good corrosion resistance of Zn-V_2O_5 composite coatings obtained at the current density 4 A dm^{-2}.

Acknowledgments

The authors are grateful to University Grant Commission and Department of Science and Technology, New Delhi, India for providing instrumental facilities. The authors wish to thank Kuvempu University, Shankaragatta, India for providing laboratory facilities to carry out this work.

References

1. A. Brenner, *Electrodeposition of Alloys, Principles and Practice*, Academic press, New York, 1963, p 80
2. E. Beltowska-Lehman, P. Ozga, Z. Swiatek, and C. Lupi, Electrodeposition of Zn-Ni Protective Coatings from Sulfate-Acetate Baths, *Surf. Coat. Technol.*, 2002, **151**, p 444–448
3. M.M. Yunan, Electrodeposition of Ternary Zinc-Nickel-Cobalt Alloys from Acidic Chloride Bath, *Met. Finish.*, 2000, **98**(10), p 38–42
4. M. Mouanga, L. Ricq, J. Douglade, and P. Bercot, Corrosion Behaviour of Zinc Deposits Obtained Under Pulse Current Electrodeposition: Effects of Coumarin as Additive, *Corros. Sci.*, 2009, **51**(3), p 690–698
5. S. Hashimoto and M. Abe, The Characterization of Electrodeposited Zn-SiO_2 Composites Before and After Corrosion Test, *Corros. Sci.*, 1994, **36**(12), p 2125–2137
6. T.J. Tuaweri and G.D. Wilcox, Behaviour of Zn-SiO_2 Electrodeposition in the Presence of *N*,*N*-Dimethyldodecylamine, *Surf. Coat. Technol.*, 2006, **200**(20), p 5921–5930
7. B.M. Praveen, T.V. Venkatesha, Y. Arthoba Naik, and K. Prashantha, Corrosion Studies of Carbon Nanotubes—Zn Composite Coating, *Surf. Coat. Technol.*, 2007, **201**, p 5836–5842

8. O. Satoshi, N. Hiroaki, K. Shigeo, A. Tetsuya, F. Hisaaki, and O. Kazuo, Electrodeposition of Zn-AlO_2O_3 Composite from Non-suspended Solution Containing Quaternary Ammonium Salt, *Hyomen Gijutsu*, 2002, **53**(12), p 920–925
9. X. Xia, I. Zhitomirsky, and J.R. McDermid, Electrodeposition of Zinc and Composite Zinc-Yttria Stabilized Zirconia Coatings, *J. Mater. Process. Technol.*, 2009, **209**(5), p 2632–2640
10. A. Gomes, M.I. da Silva Pereira, M.H. Mendonca, and F.M. Costa, Zn-TiO_2 Composite Films Prepared by Pulsed Electrodeposition, *J. Solid State Electrochem.*, 2005, **9**, p 190–196
11. B.M. Praveen and T.V. Venkatesha, Electrodeposition and Properties of Zn-Nanosized TiO_2 Composite Coatings, *Appl. Surf. Sci.*, 2008, **254**(8), p 2418–2424
12. Y.C. Lin and J.G. Duh, Effect of Surfactant on Electrodeposited Ni-P Layer as an Under Bump Metallization, *J. Alloys Compd.*, 2007, **439**(1), p 74–80
13. E. Gomez, S. Pane, X. Alcobe, and E. Vallés, Influence of a Cationic Surfactant in the Properties of Cobalt-Nickel Electrodeposits, *Electrochim. Acta*, 2006, **51**(16), p 5703–5709
14. M.-D. Ger, K.-H. Hou, and B.-J. Hwang, Transient Phenomena of the Codeposition of PTFE with Electroless Ni-P Coating at the Early Stage, *Mater. Chem. Phys.*, 2004, **87**(1), p 102–108
15. S.T. Aruna, C.N. Bindu, V. Ezhil Selvi, V.K. William Grips, and K.S. Rajam, Synthesis and Properties of Electrodeposited Ni/Ceria Nanocomposite Coatings, *Surf. Coat. Technol.*, 2006, **200**(24), p 6871–6880
16. M. Mouanga, L. Ricq, G. Douglade, J. Douglade, and P. Bercot, Influence of Coumarin on Zinc Electrodeposition, *Surf. Coat. Technol.*, 2006, **201**(3), p 762–767
17. Kh.M.S. Youssef, C.C. Koch, and P.S. Fedkiw, Improved Corrosion Behavior of Nanocrystalline Zinc Produced by Pulse-Current Electrodeposition, *Corros. Sci.*, 2004, **46**(1), p 51–64
18. J. Fustes, A. Gomes, and M.I. da Silva Pereira, Electrodeposition of Zn-TiO_2 Nanocomposite Films-Effect of Bath Composition, *J. Solid State Electrochem.*, 2008, **12**, p 1435–1443
19. S.H. Kim, H.J. Sohn, Y.C. Joo, Y.W. Kim, T.H. Yim, H.Y. Lee, and T. Kang, Effect of Saccharin Addition on the Microstructure of Electrodeposited Fe-36 wt.% Ni Alloy, *Surf. Coat. Technol.*, 2005, **199**(1), p 43–48
20. R. Ramanauskas, P. Quintana, L. Maldonado, R. Pomes, and M.A. Pech-Canul, Corrosion Resistance and Microstructure of Electrodeposited Zn and Zn Alloy Coatings, *Surf. Coat. Technol.*, 1997, **92**(1), p 16–21
21. F. Hou, W.H. Wang, and H. Guo, Effect of the Dispersibility of ZrO_2 nanoparticles in Ni-ZrO_2 Electroplated Nanocomposite Coatings on the Mechanical Properties of Nanocomposite Coatings, *Appl. Surf. Sci.*, 2006, **252**(10), p 3812–3817
22. C. Muller, M. Sarret, and M. Benballa, ZnNi/SiC Composites Obtained from an Alkaline Bath, *Surf. Coat. Technol.*, 2002, **162**(1), p 49–53
23. N.S. Qu, D. Zhu, and K.C. Chan, Fabrication of Ni-CeO_2 Nanocomposite by Electrodeposition, *Scripta Mater.*, 2006, **54**(7), p 1421–1425